

Modelling nitrate uptake and N dynamics in winter oilseed rape ([i]Brassica napus L.[/i]) during the growth cycle

Philippe P. Malagoli, Frédéric F. Meuriot, Philippe P. Laine, Erwan E. Le Deunff, Alain A. Ourry

▶ **To cite this version:**

Philippe P. Malagoli, Frédéric F. Meuriot, Philippe P. Laine, Erwan E. Le Deunff, Alain A. Ourry. Modelling nitrate uptake and N dynamics in winter oilseed rape ([i]Brassica napus L.[/i]) during the growth cycle. Quantifying and understanding plant nitrogen uptake for systems modeling, CRC Press, 320 p., 2008, 978-1420052954. hal-00964533

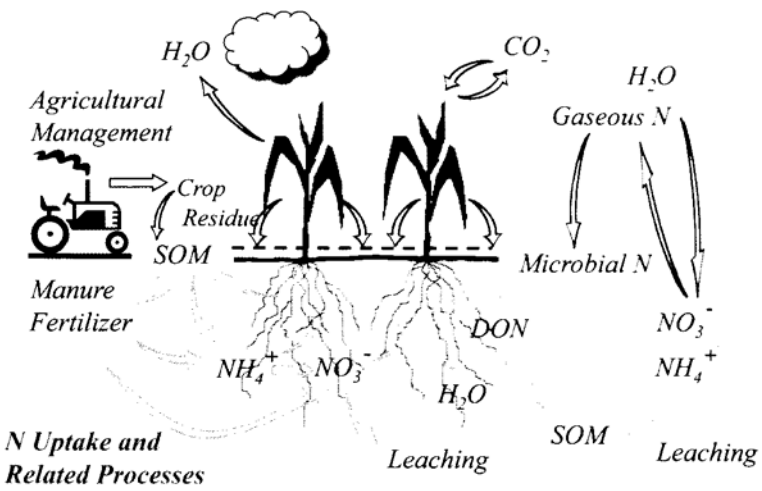
HAL Id: hal-00964533
https://hal.science/hal-00964533

Submitted on 6 Jun 2020

HAL is a multi-disciplinary open access archive for the deposit and dissemination of scientific research documents, whether they are published or not. The documents may come from teaching and research institutions in France or abroad, or from public or private research centers.

L'archive ouverte pluridisciplinaire **HAL**, est destinée au dépôt et à la diffusion de documents scientifiques de niveau recherche, publiés ou non, émanant des établissements d'enseignement et de recherche français ou étrangers, des laboratoires publics ou privés.

Quantifying and Understanding Plant Nitrogen Uptake for Systems Modeling



Edited by
Liwang Ma
Lajpat R. Ahuja
Thomas W. Bruulsema

CRC Press
Taylor & Francis Group

3 Modeling Nitrate Uptake and Nitrogen Dynamics in Winter Oilseed Rape (*Brassica napus* L.)

Philippe Malagoli, Frédéric Meuriot, Philippe Laine, Erwan Le Deunff, and Alain Ourry

CONTENTS

3.1 Introduction 48
3.2 Experimental and Modeling Methods 50
3.2.1 Growth Conditions 50
3.2.1.1 Controlled Conditions 50
3.2.1.2 Field Conditions 51
3.2.2 Experimental Design 51
3.2.2.1 Experimental Treatments for NO_3^- Influx Measurements 51
3.2.2.2 Experimental Treatment, Labeling, and Harvest for Field 52
3.2.3 Analysis and Computing Methods 52
3.2.3.1 Total Nitrogen and Isotopic Analyses 52
3.2.3.2 N Flow Calculations for the Field Experiment 52
3.2.4 Modeling Method 53
3.2.4.1 Kinetic Equations of Nitrate Transport Systems 53
3.2.4.2 Endogenous and Environmental Effects on HATS and HATS+LATS 54
3.2.4.3 Introduction of Auxiliary Variables in the Model 54
3.2.4.4 Calculation of Unregulated and Regulated Uptake 54
3.2.4.5 Sources of Input Variables 55
3.2.4.6 Basic Assumptions for Model Construction 55
3.3 Results and Discussion 56
3.3.1 Kinetics of NO_3^- Influx 56
3.3.1.1 In Induced and Noninduced Plants 56
3.3.1.2 Effects of N Deprivation on Influx Rates and Gene Expression 58
3.3.2 Modeling NO_3^- Uptake during the Growth Cycle 58

3.3.2.1 Effect of Light/Darkness Cycle and PAR on NO_3^- Influx 58
3.3.2.2 Effect of Root Temperature on NO_3^- Influx 60
3.3.2.3 Effect of Ontogeny on NO_3^- Influx 60
3.3.2.4 Cumulative Effect of Regulative Variables and Impact of N Fertilization Levels on N Uptake 61
3.3.3 Partitioning of N Uptake and N Remobilization to Vegetative and Reproductive Tissues 62
3.3.3.1 Partitioning of Uptaken N 62
3.3.3.2 Partitioning of Mobilized N 65
3.3.3.3 Mobilization of N between Senescing Leaves and the Need for a Compartmental Model 65
3.4 Conclusion 66
References 67

3.1 INTRODUCTION

Nitrogen (N) represents a central element involved in most important physiological plant processes (growth and development, photosynthesis, enzymatic functions). Limited availability of nitrogen within intensive agrosystems frequently leads farmers to apply additional N fertilizer amounts to avoid any N deficiency and depressed crop yield. However, both the N fertilization rate and schedule have to accurately match crop N demand along the growth cycle to minimize leaching losses and subsequent pollution of the wider environment (Boelcke et al. 1991; Sieling and Christen 2001).

Because of its widespread use in human (oil) and animal-centered (high-protein-content seed residues) food industry and more recently as a biofuel, the area of winter oilseed rape culture has greatly increased in Northern Europe, especially in France, and in China over the last decade. From an agronomical viewpoint, *Brassica napus* L. is commonly cycled in cereal crop rotations as a valuable break crop. Winter oilseed rape culture is also well known for its high capacity to take up mineral N from the soil. Accordingly, it is widely used as a catch/cover crop to reduce nitrate leaching from arable cropping systems during autumn and early winter (Boelcke et al. 1991; Sieling and Christen 2001). Nonetheless, despite oilseed rape's high nitrate-uptake capacity, yields are often far below those expected with such high N application rates (up to 150 kg $N \cdot ha^{-1}$ applied for a seed yield averaging 3 $t \cdot ha^{-1}$) when compared with cereal yields with similar applied N input levels. Typically, less than 50% of the applied N fertilizer is recovered in the harvested seeds (Boelcke et al. 1991). This low N recovery rate suggests that a significant N amount still remains in vegetative tissues at harvest and in the soil and is ultimately released back to the environment. This plant N release from oilseed rape occurs primarily during spring and fall, when leaves contain high amounts of N (usually more than 2% of their dry weight [DW], compared with wheat's minimal leaf N content, which is less than 1% (Schjoerring et al. 1995). In fact, it is well established that a discrepancy occurs for N remobilization in vegetative tissues until the pod-filling stage in *B. napus* L. (Malagoli et al. 2005a). Moreover, whether this high amount of N remaining in the leaves is due to an early leaf fall (i.e., source limitation) or to an incomplete N mobilization (sink-strength limitation) is still unclear.

This issue needs to be addressed to improve the N use efficiency (NUE) of winter oilseed rape crop (Schjoerring et al. 1995). For example, it can be questioned whether increased N storage capacity into buffer compartments (such as stem and taproot) would improve leaf N remobilization efficiency, which would allow matching of the seed N demand. Currently, data on the internal allocation patterns of N taken up within winter rape remains relatively scarce. Further, it is likely that the interrelationships of N flows between many N source sinks will be complex, varying both ontogenetically and along the main plant axis. It is still not known how a given leaf behaves in terms of dependence on N newly taken up (and subsequent allocation) or to remobilized N from other tissues, and how these processes are affected by leaf nodal position within the stem, i.e., its trophic nodal position (insertion in source/sink network) as well as by environmental conditions (i.e., light and temperature).

Crop-level models have already been built to predict N uptake and dynamics in winter oilseed rape (Gabrielle et al. 1998). They usually rely on a demand/supply scheme, where plant N supply is predicted from both soil N concentration and active/diffusive mechanisms. Plant N demand is usually based on a growth-rate-driven equation. While a plant N dilution curve may provide the most generic description of plant N demand, this concept may not be relevant when high N rates are applied to the soil (Gabrielle et al. 1998). Indeed, this demand/supply scheme does not take into account root physiological processes involved in both N uptake and associated regulations. Thus, it has been shown that maximal rate of nitrate root uptake in *B. napus* far exceeds that of many other cultivated species (Lainé et al. 2002). Based on physiological studies and kinetic equations, Forde (2002) reported that four main classes of nitrate transport systems are involved in nitrate root uptake in oilseed rape, namely, low- or high-affinity transport systems (LATS and HATS) with a constitutive (CHATS, CLATS) or an inducible (IHATS, ILATS) component.

Many studies have established that some plant metabolites (amino acids, nitrate, sugars, etc.) up- and/or down-regulate LATS or HATS activities and/or corresponding nitrate transporter gene expression under controlled conditions (Touraine et al. 2001). However, no study has yet predicted to what extent changes of environmental factors would quantitatively and qualitatively alter the relative contribution of each N transport system to total N uptake during plant development at the whole plant or field level. For instance, how N fertilization rates would affect the contribution of individual N transport systems, if any, under natural conditions remains unknown (Huang et al. 1999; Ono et al. 2000; Fraisier et al. 2001). This lack of knowledge led us to propose a novel N-uptake model to provide a mechanistic and powerful tool linking and extending recent molecular and physiological advances in N transport system regulation (Schjoerring et al. 1995).

To achieve this goal, the effect of several environmental (low root temperature and photosynthetically active radiation [PAR]) and endogenous factors (day/night cycle and ontogenetic stages) on HATS and LATS activities were determined by measuring ^{15}N influx under controlled conditions. Associated response curves were described and combined with basic kinetic equations in the model. The availability of independent field experimental data (from the INRA Oilseed Rape databank; http://www.bioclim.inra.grignon.fr) provided model inputs to enable simulation of N uptake by a winter oilseed rape crop during the whole growth cycle. The model

reliability (i.e., model structure and assumptions) was then evaluated by comparing model outputs with harvested exported N by this crop under field conditions. Finally, simulations through this field-level mechanistic model gave a unique chance to assess (a) the contribution of each nitrate (NO_3^-) transport system to total N uptake with increasing N fertilizer application rates, (b) the impact of each environmental or endogenous factor on N uptake during the growth cycle, and (c) the sensitivity of key model parameters regulating plant N acquisition.

3.2 EXPERIMENTAL AND MODELING METHODS

All treatments that were experimentally used—^{15}N labeling procedures, mass spectrometry analysis, and associated methods—have been previously described (Malagoli et al. 2004). Analysis of gene expression is detailed in Faure-Rabasse et al. (2002) and Beuve et al. (2004). Data from field experiments were extracted from results published by Noquet et al. (2003) and Malagoli et al. (2004, 2005a, 2005b), the latter explaining precisely how modeling of nitrate uptake was performed. They are summarized in the following subsections.

3.2.1 Growth Conditions

3.2.1.1 Controlled Conditions

3.2.1.1.1 Kinetics of NO_3^- Uptake, Light/Darkness, Temperature, and PAR Effect Experiments

Seeds of *Brassica napus* L. cv. Capitol were germinated and grown in hydroponic solution (25–50 seedlings per plastic tank) in a greenhouse in 1999. The aerated nutrient solution contained 1 mM KNO_3 (except for experimental plants used for establishing kinetics), 0.40 mM KH_2PO_4, 1.0 mM K_2SO_4, 3.0 mM $CaCl_2$, 0.50 mM $MgSO_4$, 0.15 mM K_2HPO_4, 0.20 mM Fe-Na EDTA, 14 μM H_3BO_3, 5.0 μM $MnSO_4$, 3.0 μM $ZnSO_4$, 0.7 μM $CuSO_4$, 0.7 μM $(NH_4)_6Mo_7O_{24}$, and 0.1 μM $CoCl_2$ and was renewed every two days. pH was maintained at 6.5 ± 0.5 by adding $CaCO_3$ (200 mg L^{-1}). The natural light was supplemented with phytor lamps (150 μmol m^{-2} s^{-1} of photosynthetically active radiation at the height of the canopy) for 16 h per day. The thermoperiod was 24°C ± 1°C (day) and 18°C (night).

3.2.1.1.2 N-Deprivation Experiment

Seeds were sown into six culture units (three plants/unit) of a flowing solution culture (FSC) system incorporating automatic control of concentrations of NO_3^-, K^+, and H^+ in solution (Clement et al. 1974; Hatch et al. 1986). Nutrient concentrations in each culture unit were initially (μM): NO_3^-, 250; K^+, 250; $H_2PO_4^-$, 50; Mg^{2+}, 100; SO_4^{2-}, 325; Fe^{2+}, 5.4, with micronutrients as previously described by Clement et al. (1974). Nutrient solutions were drained and refilled until day 18. Then the nutrient solution was allowed to deplete by plant uptake until day 24. From this date, K^+ concentrations were maintained at 20 ± 2 μM, and other nutrients (except NO_3^-) were supplied automatically in fixed ratios to the net uptake of K^+, for 1 mol of K, 0.645 and for 0.057, 0.045, 0.00075, and 0.522 mol of S, Mg, P, Fe, and Ca, respectively. Micronutrients were supplied as described by Clement et al. (1974). An external

NO_3^- concentration of 20 ± 2 µM was maintained automatically in each culture unit from day 24 until the start of the N-deprivation period (day 26).

3.2.1.1.3 Developmental Stage Effect Experiment

Seeds of *Brassica napus* L. cv. Capitol plants were taken from a field plot located in Saint-Aubin d'Arquenay (Normandy, France) when they were vernalized at the three-to-four-leaf stage. Plants with a well-developed taproot were harvested cautiously at the bolting stage (three to four leaves), taking care not to damage the root system. The roots were gently rinsed with deionized water before their transfer to a hydroponic system, and plants were then grown in the greenhouse as previously described.

3.2.1.2 Field Conditions

A winter oilseed rape crop (*Brassica napus* L. cv. Capitol) was sown on a clay loam soil on 10 September 2000 at Hérouvillette, 10 km north of Caen (49"10' N, 00"27' W), France. Nitrogen fertilizer was applied as NH_4NO_3 at the start of stem extension (GS 2.5; 75 kg N ha^{-1}) and at the bud visible stage (GS 3.3; 150 kg N ha^{-1}). Soil N was in excess, and water stress was not observed during the experimental period due to regular rainfall during spring. Plant density was 37–40 plants m^{-2} during the experiment (from stem extension to harvest).

3.2.2 Experimental Design

3.2.2.1 Experimental Treatments for NO_3^- Influx Measurements

Different experimental treatments (i.e., N deprivation, light/darkness cycle, low root temperatures, ontogenetic effect during the growth cycle, and photosynthetically active radiation) were realized for NO_3^- influx measurements.

When a factor was tested on NO_3^- uptake, the others remained constant during the experiment, except for the day/night cycle experiment. The thermoperiod was 20°C and 15°C during the light and the dark periods, respectively. Given that temperature had no effect on NO_3^- uptake between 15°C and 20°C, it can be assumed that its incidence on NO_3^- uptake was limited during the light/darkness cycle experiment.

NO_3^- influx rate was measured from (a) three batches of 50 seedlings (kinetics of NO_3^- uptake) or 25 seedlings (day/night cycle, low temperature, and PAR effect), (b) from six batches of three plants (N deprivation), and (c) from six plants (ontogenetic effect). The root system was rinsed twice with 1 mM $CaSO_4$ solution for 1 min and then placed in a complete nutrient solution for 5 min containing either 100 µM or 5 mM $K^{15}NO_3^-$ (^{15}N excess of 99%). For the kinetics of the NO_3^- uptake-related experiment, nitrate concentrations ranged from 0 to 7.5 mM (10, 25, 50, 75, 100, 135, 250, 1000, 2500, 5000, 7500 µM). The extent of NO_3^- depletion from these solutions during the influx assays was less than 4% in each case. At the end of feeding, roots were given two 1-min washes in 1 mM $CaSO_4$ at 4°C before being harvested. At harvest, shoots and roots were sampled separately, weighed, dried, ground into a fine powder, and kept in a vacuum with $CaCl_2$ until total nitrogen and isotopic analyses. For the experiment to measure the ontogenetic effect, the root system of harvested plants was separated into taproot and lateral roots.

3.2.2.2 Experimental Treatment, Labeling, and Harvest for Field

The ^{15}N labeling experiment was performed from stem extension (at the beginning of March) to seed maturity (at the beginning of July). Seven days before each weekly harvest date, 12 plants at the same developmental stage were randomly selected within the canopy. The petiole of each senescing leaf was attached to the stem by a nylon thread to facilitate collection of the fallen leaves. Then, 750 mL of labeled nitrogen (1 mM $K^{15}NO_3$, ^{15}N excess = 10%) was applied to the soil surface (about 400 cm^2) around each plant. Seven days after ^{15}N labeling, the plants were harvested and the root system in the top 30-cm layer of the soil was recovered carefully. The 12 plants were pooled in three sets of four plants. At each harvest, the plants were separated into lateral roots, taproot, green and dead leaves, stem, flowers, and pods. However, because of the difficulty in recovering lateral roots quantitatively under field conditions, this component was omitted from further analysis. The green leaves were numbered and then sampled individually as a function of their insertion along the stem, measured by counting leaf scars.

3.2.3 Analysis and Computing Methods

3.2.3.1 Total Nitrogen and Isotopic Analyses

Total nitrogen and ^{15}N in the plant samples were determined with a continuous flow isotope mass spectrometer (Twenty-twenty, PDZ Europa Scientific Ltd., Crewe, U.K.) linked to a C/N analyzer (Roboprep CN, PDZ Europa Scientific Ltd., Crewe, U.K.). Influx of NO_3^- was calculated from ^{15}N contents of roots and shoots.

3.2.3.2 N Flow Calculations for the Field Experiment

Dry weights and N contents of each tissue were subjected to polynomial regression ($r^2 \geq 0.90$) to minimize variation between each harvest date, and N uptake was estimated from the difference in plant N content between two harvest times. The partitioning of absorbed N was calculated from the excess ^{15}N in each tissue combined with the previously calculated total plant N uptake. Based on the assumption that unlabeled N from the soil was taken up and allocated in different plant tissues in a similar way to labeled N, the real N uptake by each tissue could be calculated as

$$\frac{(N_{d+7\text{days}} - N_d) \times {}^{15}\text{N excess in each tissue}}{\text{total } {}^{15}\text{N excess in plant}}$$

where

N_d = total nitrogen content of the plant (mg per plant) at day d when ^{15}N fertilizer was applied

$N_{d+7\text{days}}$ = total nitrogen content in the plant (mg per plant) at time d+7 days after ^{15}N fertilizer was applied

After calculating the N in each organ derived from uptake, the pattern of net translocation of endogenous unlabeled N (N absorbed before the beginning of labeling) among plant parts could be used to estimate N mobilization within the plant. At

each harvest, the amount of N mobilized from or to each tissue (N_{mob}) was calculated by subtracting the total amount of N ($N_{d+7days}$) from (a) the N derived from uptake (N uptake) and (b) the previous amount of N in this tissue seven days before (N_d):

$$N_{mob} = N_{d+7days} - N_d - \text{N uptake}$$

Thus positive values of N_{mob} represent nitrogen that was mobilized to the tissue, whereas negative values correspond to a net mobilization of N from the tissue. For each leaf insertion, the following values were calculated:

1. The cumulative amounts of both N derived from N taken up, and endogenous N mobilized from source tissues
2. Percentage of mobilization of N = $(N_{max} - N_{min}) \times 100/N_{max}$, where N_{max} and N_{min} correspond to the highest and lowest values of total nitrogen (mg per plant), respectively
3. Dates of appearance, loss or abscission, and start of mobilization of endogenous N (calculated when N mobilization reached negative values) expressed in thermal time (°C days)

3.2.4 Modeling Method

A mechanistic single-root model that explains nitrate uptake of plants mainly based on NO_3^- concentration around the root system was developed. The proposed thermal time-step model simulates total NO_3^- uptake by rape crops from the root transport processes formalized by kinetic equations of the different NO_3^- transport systems involved in N uptake.

3.2.4.1 Kinetic Equations of Nitrate Transport Systems

Faure-Rabasse et al. (2002) have determined the kinetics of the constitutive and inducible components of HATS and HATS+LATS in 15-day-old seedlings of rape using ^{15}N labeling experiments. These authors demonstrated that influx rates approximated Michaelis–Menten kinetics below 200 µM (CHATS, IHATS), while at higher NO_3^- concentrations (>1 mM), influx rates of CHATS+CLATS and IHATS+ILATS exhibited nonsaturable kinetics. A Michaelis–Menten-type equation ($I = I_m \times [NO_3^-]/([NO_3^-] + K_m)$ where I = nitrate influx rate; I_m = maximum nitrate influx rate; K_m = affinity constant) for HATS components (constitutive and inducible) and linear equations ($I = a \times [NO_3^-] + b$; a, b are constants) for HATS+LATS constitutes the basis of the model. Influx values of CLATS and ILATS were estimated in our model by subtracting the I_m value of CHATS and CHATS+CLATS influx and IHATS from IHATS+ILATS influx, respectively. It is noteworthy that LATS is considered to operate when soil NO_3^- concentration is above 900 µM and 1 mM for the CLATS and ILATS, respectively. At lower NO_3^- concentrations, LATS activities were integrated into the functioning of HATS because it is not physiologically possible to distinguish the HATS and LATS activities. Indeed, only the use of LATS mutants would allow quantification of the real contribution of LATS under 1 mM of NO_3^-, as previously reported (Wang et al. 1998; Liu et al. 1999).

3.2.4.2 Endogenous and Environmental Effects on HATS and HATS+LATS

The response curves of the effects of different factors such as the light/darkness cycle (16/8 h), ontogeny, application of low temperatures (from 24°C to 4°C) to the root system, or variations of photosynthetically active radiation (from 0 to 500 µmol m^{-2} s^{-1}) on HATS and HATS+LATS activities were obtained by measuring NO_3^- influx at 100 µM and 5 mM $K^{15}NO_3$, respectively. This made it possible to calculate HATS (CHATS+IHATS) activities at the initial concentration (100 µM) and LATS (CLATS+ILATS) activities from the difference in uptake rates measured for the two substrate concentrations used. Variations of influx for each transport system as a function of the studied factors were subsequently fitted with polynomial equations.

3.2.4.3 Introduction of Auxiliary Variables in the Model

Environmental and endogenous factors, introduced into the model as auxiliary variables, allowed integration of regulations by N demand on NO_3^- uptake. Indeed, light/darkness cycle and ontogeny were chosen and incorporated into the model in order to take short- (light/darkness cycle) and long-term (ontogeny) regulations acting on N transport systems into account. Environmental variables such as temperature and radiation were introduced because of their well-known impact on growth and N uptake. Consequently, endogenous factors can be considered as "metaregulation mechanisms" that are influenced by climatic factors (PAR and temperature) permitting access to a higher level of nitrate-uptake regulation by N demand.

To integrate the effects of these different factors on HATS and HATS+LATS activities, a standard influx (SI) value was determined for each studied factor: $SI_{light-darkness}$, $SI_{ontogeny}$, $SI_{temperature}$, and SI_{PAR}. Each value was defined for the following conditions: 12 p.m. for a light/darkness cycle of 16/8 h, 20°C for root temperature, 300 µmol s^{-1} m^{-2} for PAR, and B4 stage for ontogeny (i.e., four-leaf stage). These conditions were similar to those used by Faure-Rabasse et al. (2002) to determine nitrate influx kinetics. Because effects of these factors were measured in different experiments, SI values allowed us to adjust the fluctuations of measured influx between these experiments. Thus, a corrected influx (CI) was determined for each factor studied by application of a correction factor defined as the ratio between the value of nitrate influx, obtained by the above-cited adjusted polynomial equations (section 3.2.4.2), and the SI value for each studied factor. For example, the average influx values per day (1884 and 4889 µmol NO_3^- d^{-1} g^{-1} root DW for HATS and HATS+LATS, respectively) obtained by integrating equations for HATS and for LATS from 0 to 24 hours were divided by respective $SI_{light/darkness}$ values. (For detailed equations, see Malagoli et al. 2004.)

3.2.4.4 Calculation of Unregulated and Regulated Uptake

An unregulated uptake (expressed in kg $N\text{–}NO_3^-$ ha^{-1}) was calculated from kinetic equations by taking into account soil nitrate concentration and root biomass at different depths and plant densities throughout the growth cycle, and by operating a change of time scale (from hours to days) by multiplying by 24.

The regulated uptake in the model was determined by multiplying the kinetic equations by correction factors. Integration of light/darkness and ontogenetic cycle

factors allowed a change of time scale from hour to day and from days to growth cycle, respectively. The last auxiliary variables, temperature and PAR, were then integrated to simulate NO_3^- uptake in environmental field conditions. Changes in day length (minutes) during the year were also taken into account in the model with a day-length reference value equal to 960 min.

3.2.4.5 Sources of Input Variables

Input variables (soil nitrate concentrations and root biomass at different soil depths, temperature, and PAR) needed to run the model were obtained from the INRA oilseed rape database of experiments carried out at Grignon/Châlons/Laon/Reims (http://www-bioclim.inra.grignon.fr). Details about these experiments can be found in Gosse et al. (1999).

The main difficulty encountered when running the model was to estimate the lateral root biomass, which was assumed to be the only part of the root system involved in N uptake, this assumption being based on the fact that NO_3^- uptake by the taproot was found to be insignificant (about 1%, unpublished results). Independently of the studied developmental stage, previous experiments carried out under controlled conditions have shown that lateral root biomass represents an approximately constant proportion of 43% of the total root biomass (taproot + lateral root). This value was introduced as a parameter (p) in the model. To estimate lateral root biomass, a pattern of lateral root biomass distribution among soil layers was estimated from the frequencies of lateral root impact as a function of soil depth available in the database. Using this distribution and the total calculated lateral root biomass, lateral root biomass in each soil layer was assessed. Nitrogen uptake (kg ha^{-1}) in each soil layer was obtained by multiplying the regulated uptake by the root biomass calculated in each soil layer.

Nitrate concentrations in the different soil layers were determined every 15 days using the Skalar method (Gosse et al. 1999). Soil NO_3^- limitation was defined as the maximum soil nitrate stock available for N uptake. Thus, soil nitrate limitation was calculated every 15 days over the whole growth cycle from the database corresponding to soil NO_3^- concentration and soil water content in the different soil layers and N uptake by plants between two harvest dates. An interpolation was made between these two dates.

Finally, model output (i.e., predicted N uptake by the crop) is the sum of N uptake along the root profile. This model was tested to compare observed and predicted N uptake by oilseed rape plants with three levels of N fertilization (N0: 0 kg N ha^{-1}; N1: 135 kg N ha^{-1}; N2: 273 kg N ha^{-1}). The highest soil NO_3^- concentrations were found in the first soil layer. The variation scale in this soil layer ranged from 0.23 to 4.1, from 0.15 to 4.1, and from 0.24 to 7.0 mM for N0, N1, and N2 fertilization, respectively. The model was built using Model Maker software (Cherwell Scientific, Oxford, U.K.).

3.2.4.6 Basic Assumptions for Model Construction

Both nitrate (NO_3^-) and ammonium (NH_4^+) can be used for N nutrition by many crop species. However, it has been reported that Brassicaceae are characterized as NH_4^+-

sensitive plants (see review by Britto and Kronzucker 2002). Even if NH_4NO_3 is used to fertilize plots, ammonium in the soil is readily oxidized to NO_3^- by nitrifying bacteria present in the soil. NO_3^- is the prominent form of N available to most cultivated plants grown under normal field conditions. Moreover, availability of NO_3^- in the soil is often considered as rate limiting for plant growth (Redinbaugh and Campbell 1991). For these reasons, NO_3^- was assumed to be the sole N source used for N nutrition in our work. No NO_3^- efflux was considered under field conditions. Kinetic parameters—K_m and I_m for HATS, a and b for HATS+LATS—were assumed to remain constant during a growth cycle, while NO_3^- transporters were assumed to have a homogenous spatial distribution along lateral roots. A minimum temperature of 4°C was assumed to be the lowest temperature at which growth may occur. Consequently, nitrate uptake by transport systems when temperature was below 4°C was considered as negligible.

It was hypothesized that the taproot/lateral root ratio assessed under controlled conditions was similar under field conditions and remained constant throughout the growth cycle. No competition for water, light, or mineral nutrient acquisition was considered between oilseed rape plants.

Concerning auxiliary variables, plants at the vegetative stage (B4) were used to study the effects of root temperature, light/darkness cycle, and PAR on NO_3^- uptake. Effects of these factors were formalized by polynomial equations and assumed to be the same for all developmental stages. Up- and down-regulations of nitrate transport systems that may occur at the plant level through the effects of different phloem or root compounds issued from nitrate assimilation or photosynthetic activity (amino acids, organic acids, sugars) were implicitly included through the light/darkness cycle or ontogeny. The two constitutive and inducible components of each transport system (high or low affinity) were assumed to be similarly regulated by these compounds. The effect of PAR was taken into account in the model from bolting to harvest according to Chapman et al. (1984) and Mendham et al. (1981), who have demonstrated a decrease of about 60%–80% of PAR transmitted inside the rape canopy at the beginning of flowering. No interaction between climatic factors (temperature and PAR) was taken into account.

3.3 RESULTS AND DISCUSSION

3.3.1 Kinetics of NO_3^- Influx

3.3.1.1 In Induced and Noninduced Plants

On day 15 after sowing, half of the total number of plants previously grown without N were supplied with 1 mM KNO_3 for 24 h to induce the NO_3^- uptake system. Nitrate influx rate was measured on day 16 for both induced and noninduced plants.

At least three different transport systems for NO_3^- uptake were distinguished in *Brassica napus* L. on the basis of a kinetic characterization (Figure 3.1). Two of them were constitutive systems in noninduced seedlings. For NO_3^- concentrations below 200 µM, influx rates approximated Michaelis–Menten kinetics (Figure 3.1A, CHATS), with an estimated I_{max} of 26.3 $\mu mol \cdot h^{-1} \cdot g^{-1}$ DW and a K_m of 15.9 µM. A second low-affinity system (Figure 3.1B, CLATS) exhibited nonsaturable

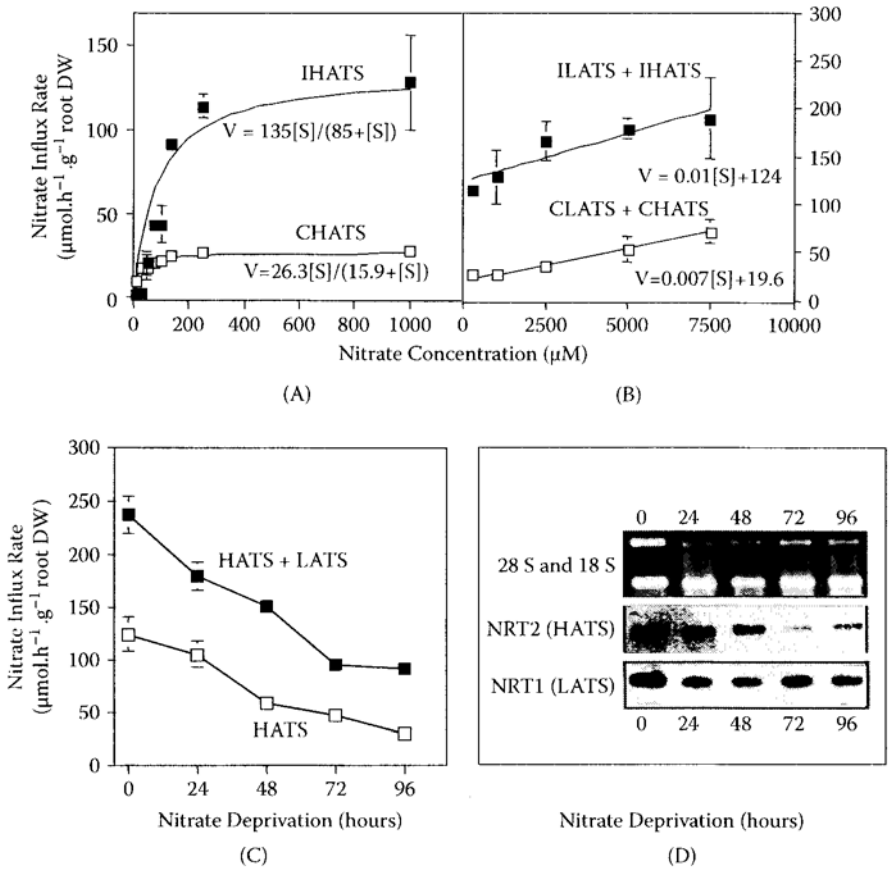


FIGURE 3.1 Kinetic analysis of ^{15}N-nitrate influx by *Brassica napus* L. roots with low (A) or high (B) nitrate concentrations in the nutrient solution. CHATS and IHATS: constitutive and inducible high-affinity transport system, respectively. CLATS and ILATS: constitutive and inducible low-affinity transport system, respectively. (C): Effect of nitrate deprivation on low (CLATS+ILATS) or high (CHATS+IHATS) affinity transport system for nitrate, estimated by ^{15}N labeling. (D): Changes in NRT1 and NRT2 gene expression estimated by Northern blotting during nitrate deprivation. [Redrawn from Faure-Rabasse et al. (2002).]

kinetics between 1 to 7.5 mM NO_3^-. When seedlings were induced by exposure to 1 mM NO_3^- for 24 h prior to assaying influx, NO_3^- uptake increased across the entire range of concentrations. The inducible high-affinity system approximated Michaelis–Menten kinetics at substrate concentrations lower than 1 mM (Figure 3.1A, IHATS), with an I_{max} of 135 μmol·h^{-1}·g^{-1} DW and a K_m of 85 μM. Nitrate influx attributable to the IHATS was fivefold higher than the one associated with the CHATS. The kinetics of NO_3^- uptake determined at high concentrations (1–7.5 mM NO_3^-) suggests that the LATS is devoid of an inducible component. These results show that a simple mathematical description (two Michaelis–Menten plus two linear equations) can be used to describe nitrate transporter activities as a function of external nitrate concentration.

3.3.1.2 Effects of N Deprivation on Influx Rates and Gene Expression

On day 26 after sowing, the automatic supply of NO_3^- was switched off to culture units, and the concentrations of NO_3^- in these units were allowed to deplete by plant uptake to <1 µM over 2 h. This point was taken as time zero for the N-deprivation treatment. NO_3^- influx and mRNA abundance were measured on N-deprived plants at intervals during the period of N deprivation (0, 24, 48, 72, and 96 h). NO_3^- influx was measured 2 h prior to the end of the photoperiod for six culture vessels per treatment.

Plant growth (i.e., dry-matter production) was not significantly affected during the first four days of NO_3^- deprivation, implying that the N deprivation effect on NO_3^- influx and gene expression during this period were unrelated to changes in rates of growth or senescence. Nitrate uptake through high-affinity systems (Figure 3.1C, 100 µM) decreased progressively over the four days of N deprivation from 125 to 30 $\mu mol \cdot g^{-1}$ root DW h^{-1}. Meanwhile, regarding the importance of HATS in total nitrate influx rate, this decrease also reduced the HATS+LATS uptake from 240 to 100 $\mu mol \cdot g^{-1}$ root DW h^{-1}. Seventy percent of this decline was observed during the first 48 h of N starvation (see Faure-Rabasse et al. 2002 for a full description). The abundance of mRNA encoding for the *BnNRT2* NO_3^- transporters (i.e., HATS) decreased as a function of the duration of NO_3^- deprivation (Figure 3.1D), demonstrating that this gene is nitrate inducible. The expression of the *BnNRT1* gene was less strongly affected by nitrate deprivation.

3.3.2 Modeling NO_3^- Uptake during the Growth Cycle

For each studied developmental stage (C2, D2, E, F2, G2, G4, G5), plants were acclimated for 1.5 h to KNO_3 concentrations (100 µM or 5 mM), as previously described, before influx measurements were made at 12 p.m.

A mechanistic model was built combining the mathematical description of NO_3^- influx kinetics (from data in Figure 3.1) and data from field experiments (root biomass, soil nitrate concentrations, temperature, PAR) obtained from the INRA Châlons Oilseed Rape database (France) to simulate NO_3^- uptake. When total N uptake was controlled only by soil NO_3^- concentrations (i.e., unregulated uptake), model outputs were largely overestimated (17 times higher) compared with the measured data. Further, nitrate systems regulations (a) occurring during the day/night cycle or during development and (b) resulting from the differential effect of temperatures or photosynthetically active radiation availability were successively introduced into the model.

3.3.2.1 Effect of Light/Darkness Cycle and PAR on NO_3^- Influx

Fifteen-day-old seedlings were transferred from the greenhouse to a culture room for one week. Light was provided by high-pressure sodium lamps (300 $\mu mol\ m^{-2}\ s^{-1}$ of photosynthetically active radiation at the height of the canopy), and the thermoperiod was 20°C (day) and 15°C (night). Before each measurement, plants were acclimated for 1.5 h in a nutrient solution containing either 100 µM or 5 mM KNO_3. NO_3^- influx was then determined at t = 3, 6, 9, and 12 h after the beginning of the diurnal period (i.e., 9 a.m., 12 p.m., 3 p.m., and 6 p.m.) and at t = 0, 2, 4, 6, and 8 h after the beginning of the dark period (i.e., 10 p.m., 12 a.m., 2 a.m., 4 a.m., and 6 a.m.). The

same procedure was undertaken for the PAR experiment, and different PAR values (ranging from 0 to 500 μmol m^{-2} s^{-1}) were obtained by varying the height between the top of the canopy and the lamps. After acclimation for 1.5 h in a nutrient solution containing either 100 μM or 5 mM KNO_3, NO_3^- influx was measured at 12 p.m.

NO_3^- influx displayed a marked diurnal cycle, as shown by minimal and maximal values reported in Figure 3.2A. From the start of the light period (6 a.m.), HATS activity increased about 1.5-fold to reach a maximum value (about 100 μmol NO_3^- g^{-1} root DW h^{-1}) at 12 p.m. By the end of the light period HATS influx then decreased progressively back to a similar value measured at the start of the light period (70 μmol NO_3^- g^{-1} root DW h^{-1}). During the dark period, HATS influx decreased to a nearly constant value of about 50 μmol NO_3^- g^{-1} root DW h^{-1}. The pattern of HATS+LATS influx exhibited two peaks (about 266 μmol NO_3^- g^{-1} root DW h^{-1}) at 9 a.m. and 6 p.m. Integration of this short-term effect was of major importance when

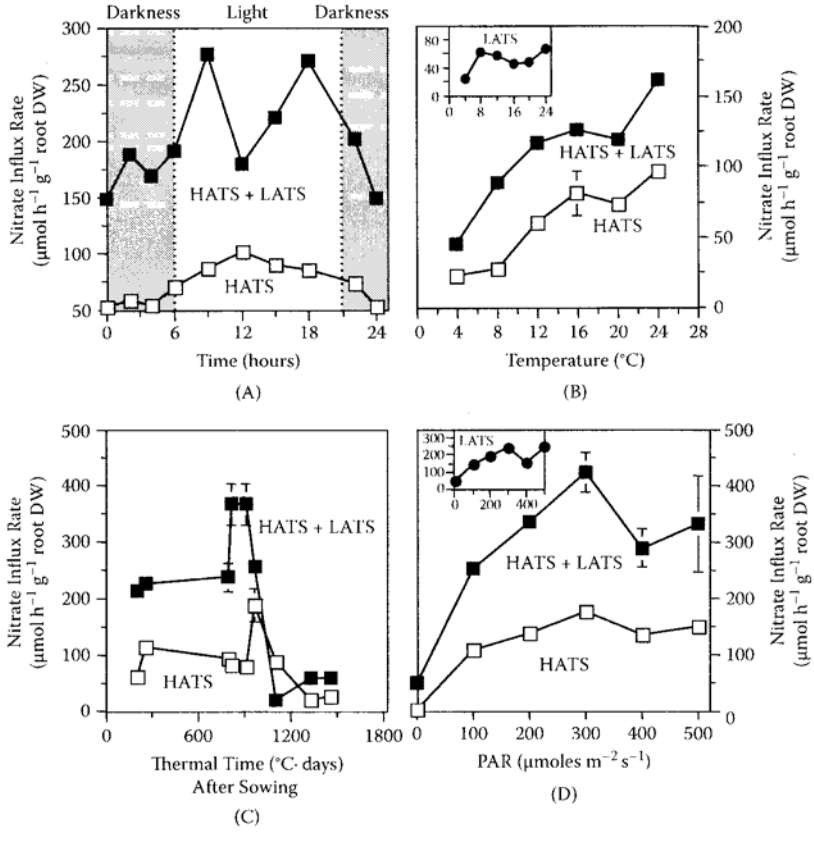


FIGURE 3.2 Variations of HATS (■) and both HATS+LATS (□) activities during the light/darkness cycle (A), as a function of root temperature (B), during a growth cycle (C), and as a function of photosynthetically active radiation (μmol m^{-2} s^{-1}) (D) in *Brassica napus* L. var. Capitol. Insets in Figures 3.2B and 3.2D represent the LATS activity, obtained by subtracting HATS activity from HATS+LATS activity. Vertical bars indicate ±SD for $n = 3$ when greater than the symbol. [Redrawn from Malagoli et al. (2004).]

scaling from hourly to daily influx, as it decreased simulated N taken up by 50%. When the day length was further taken into account, it led to a more pronounced decrease during winter, and a final 32% decrease compared with the unregulated N uptake was observed at harvest.

Light availability limitation occurs during winter (i.e., PAR intensity decreases at the canopy level) and spring (i.e., leaf, flower, pod shields [up to 80%] leading to a decreased light penetration through leaf layers within the canopy and subsequent low light radiation values for leaves). This effect becomes quite important, as a lower availability of photosynthetically active radiation will consequently down-regulate the photosynthesis and evapotranspiration, as well as decrease both the energy supply and the water fluxes to the roots, leading to reduced N-uptake capacities. It was then important to take these daily PAR variations into account and to consider changes of HATS and HATS+LATS activities as a function of PAR values (ranging from 0 to 500 μmol m^{-2} s^{-1}) (Figure 3.2D). Both HATS and HATS+LATS activities increased with PAR up to 300 μmol m^{-2} s^{-1} (from 3.7 to 177 μmol NO_3^- g^{-1} root DW h^{-1}, and from 50 to 450 μmol NO_3^- g^{-1} root DW h^{-1} for HATS and HATS+LATS, respectively). LATS activity followed the same pattern, with a saturation point (250 μmol NO_3^- h^{-1} g^{-1} root DW) at 300 μmol m^{-2} s^{-1}. When this effect was included into the model, simulated N uptake was reduced by 19%.

3.3.2.2 Effect of Root Temperature on NO_3^- Influx

Two days before the experiments, 15-day-old seedlings were transferred from the greenhouse to a control room under the previously described conditions. NO_3^- influx was measured after acclimation for 1.5 h in a nutrient solution containing either 100 μM or 5 mM KNO_3 at different root temperatures (4, 8, 12, 16, 20, and 24°C) maintained with a cryostat. All influx measurements lasted about 45 min from 12 p.m. Temperatures of the solution used for NO_3^- influx measurements were similar to those applied during the pretreatment.

The time course of the NO_3^- influx of HATS and HATS+LATS showed a similar pattern for the range of tested temperatures (from 4°C to 24°C; Figure 3.2B). However, LATS influx (obtained by subtracting HATS activity from HATS+LATS activity) was barely altered by low root temperature, except at 4°C (inset in Figure 3.2B). In addition, decreasing the root temperature from 24°C to 4°C resulted in a sharp reduction of HATS activity (from 100 to 25 μmol NO_3^- g^{-1} root DW h^{-1}). Overall results show that the N transport activities will be affected differently by temperature, the LATS being less sensitive than the HATS, i.e., when low temperatures occur in winter or in early spring. The effect of varying temperature decreased the predicted N taken up by 36%. Moreover, it was observed that the temperature factor decreased the simulated N uptake (–80%) more than the PAR and light/darkness cycle (–50%) during this period.

3.3.2.3 Effect of Ontogeny on NO_3^- Influx

The time course of the NO_3^- influx of HATS and HATS+LATS was different with developmental stages (Figure 3.2C). NO_3^- influx of both transport systems was more or less unchanged from the two-leaf stage (B2) to the bolting stage (C2) (about 130

and 240 µmol NO_3^- g^{-1} root DW h^{-1} for HATS and HATS+LATS, respectively). From the bolting stage (C2) to the initiation of bud development (E), HATS+LATS activity increased 1.4-fold, while HATS activity remained constant (about 80 µmol NO_3^- g^{-1} root DW h^{-1}; Figure 3.2C). A drastic increase of HATS influx was observed from the E stage (81 µmol NO_3^- g^{-1} root DW h^{-1}) to the F2 (flowering) stage (187 µmol NO_3^- g^{-1} root DW h^{-1}), whereas HATS+LATS influx dropped abruptly from 366 to 250 µmol NO_3^- g^{-1} root DW h^{-1}. Both HATS and HATS+LATS activities decreased thereafter to a minimal value (30 µmol NO_3^- g^{-1} root DW h^{-1}). As a consequence, it appears that both transport systems are differentially regulated during plant growth (i.e., with an up- and a down-regulation during bolting and after flowering, respectively). The latter result suggests that N content in the pods at maturity will be mostly derived from the mobilization of N previously taken up early in the growth cycle for the growth of vegetative tissues. Taking into account this long-term effect allows us to scale up from daily N uptake to the complete growth cycle. When regulations occurring simultaneously or successively on transport system activities along the whole life cycle and at the whole plant level (i.e., long-term effect) were integrated into the model, their impact was only observed at the end of the growth cycle (–24%; Figure 3.3A) during the seed-filling stage (G2 to G5).

3.3.2.4 Cumulative Effect of Regulative Variables and Impact of N Fertilization Levels on N Uptake

Both light/darkness and temperature effects were responsible for 66% of the overall decrease in predicted nitrate uptake, emphasizing the major role played by these variables on NO_3^- uptake by plants when no fertilizer (N0 treatment) was applied (Figure 3.3B). Integrating all these variables in the model resulted in a 5.8-fold reduction of the simulated total N uptake at harvest compared with the unregulated uptake (Figure 3.3B). Comparison of the amounts of the measured and the predicted N uptake at harvest shows that the simulated N uptake, defined as the regulated uptake without soil N limitation, was still three times higher than the observed N uptake, taking soil nitrate availability into account (Figure 3.3B). When the model was run with increasing N inputs (from N1 to N2 treatment), outputs showed that the model was responsive to N fertilizer application compared with the N0 treatment (Figure 3.4).

Integration of the four variables decreased the amount of simulated total N uptake by about a factor of 5.5 for N0 (Figure 3.4A) and N1 (Figure 3.4B) treatments and 3.5 for the N2 treatment (Figure 3.4C). However, an overestimation of the modeled N uptake after the flowering stage was observed for all N treatments. When plant N supply was limited by the soil N availability, the model more accurately matched measured data for N0, N1, and N2 (comparison of regulated uptake with and without soil N limitation; Figures 3.4A, 3.4B, and 3.4C). Indeed, in spite of the high potential activity of the N transport system described in the model (i.e., regulated uptake without soil N limitation), soil N supply from the start of the flowering (F2) to the pod filling (G2) stage was not sufficient to match plant N requirements. Based upon satisfactory model outputs, sensitivity analysis was then performed to identify key parameters that need to be improved through genetic engineering or better management practices (Malagoli et al. 2005b). The analysis showed that (a)

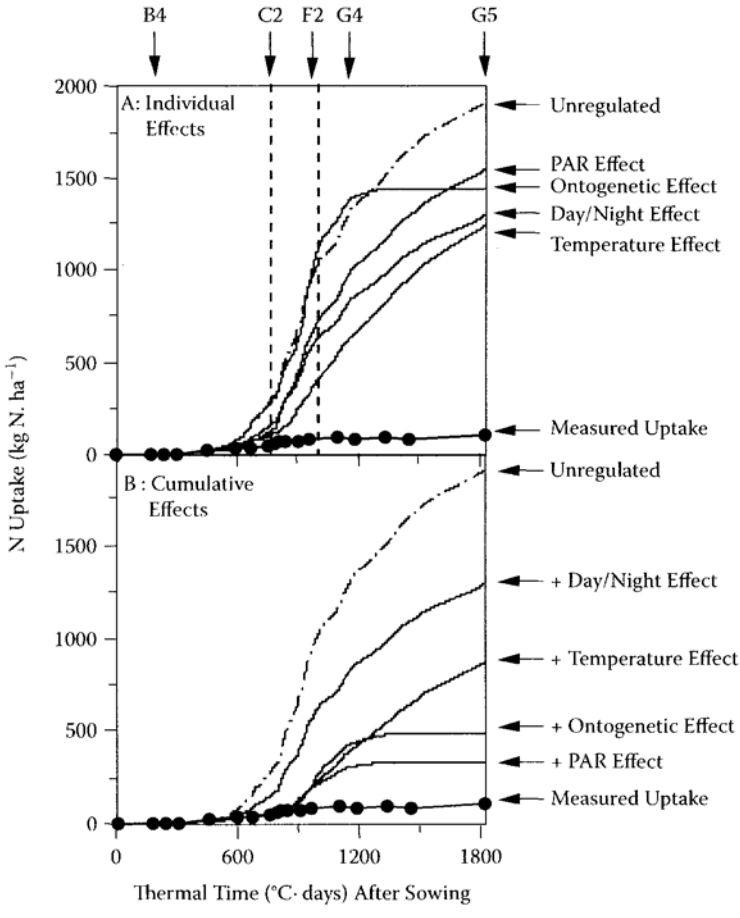


FIGURE 3.3 Simulation of N uptake by an oilseed rape crop (*Brassica napus* L. var. Capitol) with no fertilizer when introducing the impact of the light/darkness cycle, root temperature, ontogeny, and PAR effects on NO_3^- uptake during the growth cycle, either individually (A) or cumulatively (B). [Redrawn from Malagoli et al. (2004).]

the affinity constant of saturable transporters is nonlimiting within the common range of concentrations found in the field, and (b) the contribution of low-affinity nitrate transport to total N remained low and is important solely during periods of high-organic N mineralization and immediately after N fertilization.

3.3.3 Partitioning of N Uptake and N Remobilization to Vegetative and Reproductive Tissues

3.3.3.1 Partitioning of Uptaken N

A weekly $^{15}NO_3^-$ labeling under field conditions allowed us to monitor cumulative N uptake and track uptake- and remobilization-derived N into plant compartments from bolting to harvest (Figure 3.5A). The amounts of ^{15}N increased in green leaves,

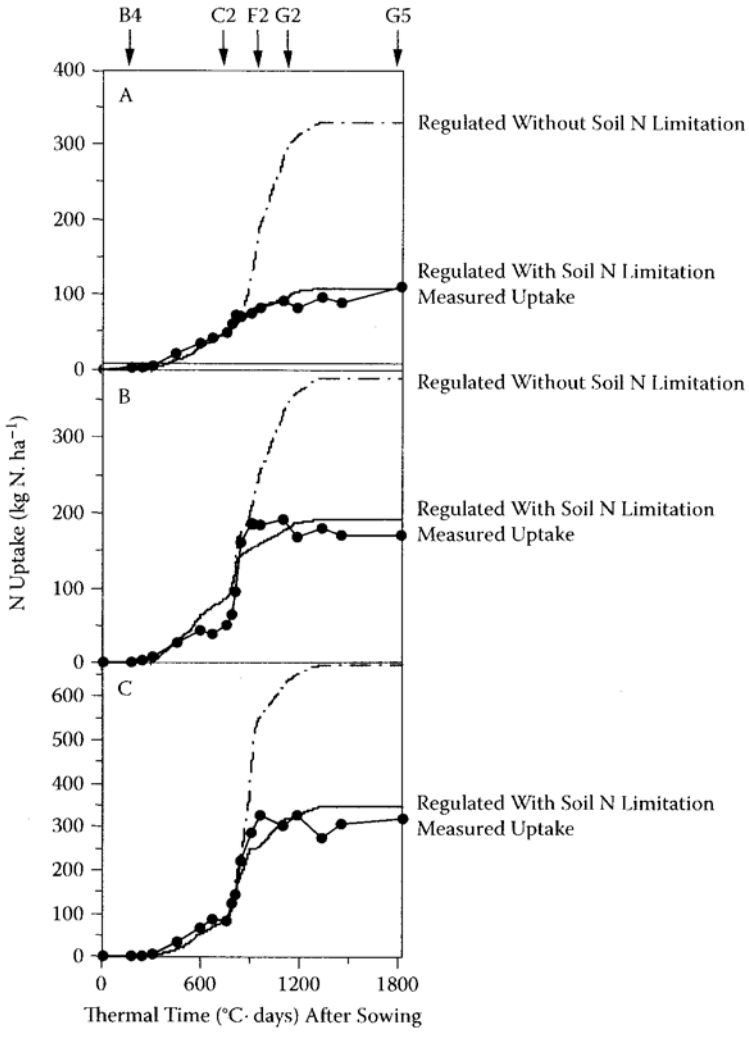


FIGURE 3.4 Simulation of N uptake by an oilseed rape crop (*Brassica napus* L. var. Capitol) with and without the soil N limitation during a growth cycle as a function of three N fertilizer levels: (A) 0 kg N ha^{-1} (treatment N0); (B) 135 kg N ha^{-1} (treatment N1); (C) 273 kg N ha^{-1} (treatment N2). [Redrawn from Malagoli et al. (2004).]

stem, taproots and flowers until the end of the flowering (F2). Nitrogen uptake and further allocation (Figure 3.5A) to taproot and flowers reflects growth, relative mass, and N content. In contrast, the green leaf compartment showed a constant increase of N allocation until the end of flowering, while its biomass remained close to a steady-state value from 1700 to 2350 °C·days. This probably reflects a high N turnover in green leaves and subsequently a high re-export of N. A similar conclusion can be made for the stem after flowering: a continuous increase of allocation of N derived from uptake (Figure 3.5), while its biomass remained the same. From the G1 stage, pods became the main organs where uptaken ^{15}N was allocated, while no significant

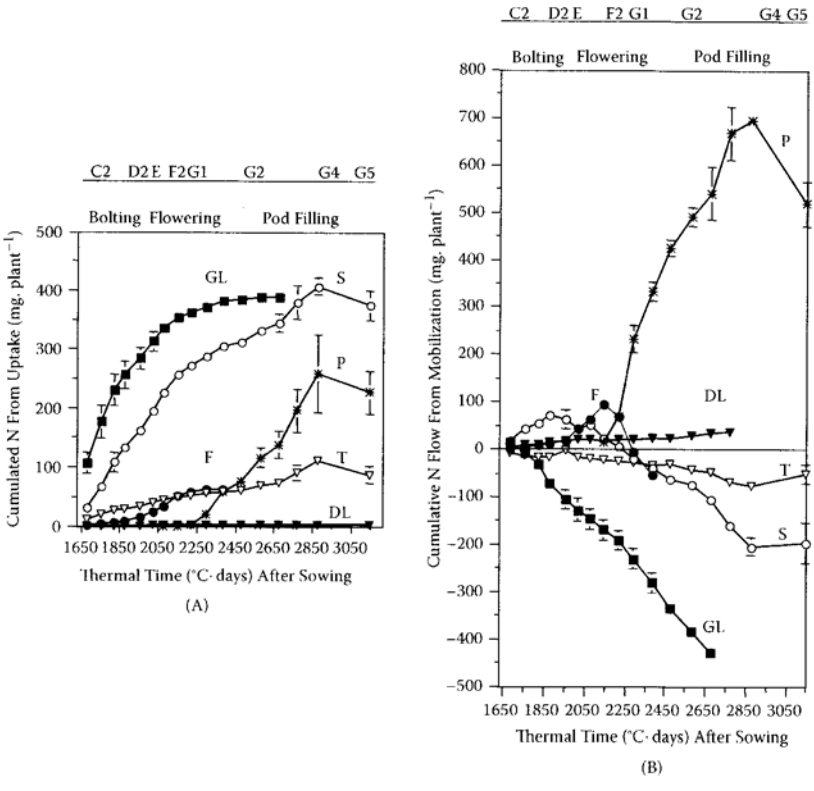


FIGURE 3.5 Cumulative N uptake, further allocation (A), and cumulative endogenous N flows (B) estimated by weekly ^{15}N labeling in *Brassica napus* L. var. Capitol plants grown under field conditions to taproot (T), green leaves (GL), dead leaves (DL), stem (S), flowers (F), and pods (P). Vertical bars indicate ±SD for $n = 3$ when larger than the symbol. [Redrawn from Malagoli et al. (2005a).]

increase in ^{15}N was observed in green leaves, although ^{15}N continued to accumulate in the stem and taproot until 2850 °C·day.

The ^{15}N flux in each organ (expressed in μg N·plant^{-1}·[°C·day]$^{-1}$), i.e., the slope of the different straight lines defined between the inflection points in each curve, was calculated to determine the rate of ^{15}N allocation associated to each compartment. From the start of bolting (C2) to the start of pod filling (G1), organs can be classed as a function of their decreasing order in priority: leaves, stem, taproot, and flowers. The amount of ^{15}N allocated to the stem was relatively constant (490 ± 13 μg N·plant^{-1}·[°C·day]$^{-1}$). In contrast, sink strength of leaves and flowers varied during bolting and flowering. From D2/E to G1, the amount of ^{15}N allocated to green leaves declined (from 1174 ± 132 during C2/D2 to 380 ± 64 μg N·plant^{-1}·[°C·day]$^{-1}$ during D2/G1) and increased in flowers (from 39 ± 7 during C2/D2 to 157 ± 9 μg N·plant^{-1}·[°C·day]$^{-1}$ during D2/G1), reflecting a switch in ^{15}N allocation priority to the benefit of the new growing sinks. During pod filling (from G1 to G5), N uptake was maintained at a significant level—30% of the total N taken up by the crop, with the pods becoming the main sink for uptaken N (Figure 3.5A).

3.3.3.2 Partitioning of Mobilized N

Taking all data together allowed us to determine endogenous N flows before and during pod filling (Figure 3.5B). An overview of source–sink relationships for N was obtained by summing endogenous N influx (positive values of N_{mob}) and efflux (negative value of N_{mob}) for each tissue, so that a sink organ for N had an increase in cumulative endogenous N flow, whereas a source organ had a decrease in cumulative endogenous N flow. Figure 3.5B illustrates the transition from sink to source behavior of a tissue when the maximum cumulative flow from remobilization is reached and then declines. This demonstrates that the leaves and the taproot, to a lesser extent, were permanent sources of endogenous N during the studied period. From the start of bolting (C2) to the visible buds stage (E), endogenous N coming from leaves and taproot were mainly allocated to the stem (86%) and later to flowers (14%), although a portion remained in dead leaves. The status of the stem changed from sink to source during floral transition at about 1850 °C·days. During the flowering period (from E to F2), flowers became the only sinks for endogenous N, supplied by the leaves (57%), the stem (38%), and the taproot (5%), before behaving as a source at 2150 °C·days. During pod filling, all vegetative tissues behave as sources for endogenous N. Indeed, about 690 mg of endogenous N were mobilized to the pods: 36%, 34%, 22%, and 8% being mobilized from leaves, stems, inflorescences, and taproot, respectively.

This N partitioning establishes for the first time that the contribution of labeled and unlabeled N flows to each tissue could be accurately determined under field conditions in *B. napus* L. Exogenous (i.e., labeled) N derived from concurrent uptake is the only source of N for a source tissue, while a sink organ will get N from concurrent uptake as well as from mobilization of N from source tissues. Endogenous (i.e., unlabeled) N represented 35%, 64%, and 73% of the total N allocated to the stem, the flowers, and the pods, respectively. Leaves were the most important source organ for endogenous N mobilization throughout the experiment, although contributions from stem and taproot increased between G3 and G4 during pod filling. Endogenous N mobilization rate was strongly increased during pod filling: in the stem (by 2.7-fold), taproot (by 2.5-fold), and to a lesser extent in the leaves (by 1.4-fold). Comparison of data for pods in Figures 3.5A and 3.5B shows that 73% of N in these reproductive tissues was derived from internal mobilization. However, it should be kept in mind that, during this field experiment, rainfall and mineral N in the soil remained relatively high, and this would probably minimize the role of internal recycling, as a significant N uptake occurred during pod development (Figure 3.5A).

3.3.3.3 Mobilization of N between Senescing Leaves and the Need for a Compartmental Model

With a large number of leaves, the oilseed rape plant represents a complex compartmental system. On a theoretical basis, it can be assumed that, within a leaf rank, changes of total N content during the leaves' life span (Figure 3.6) is a result of two incoming N fluxes of different origin—(a) the allocation of N directly derived from uptaken N, and (b) N allocated to this leaf rank that is derived from N remobilization from lower leaf insertions—and one outgoing flux corresponding to the

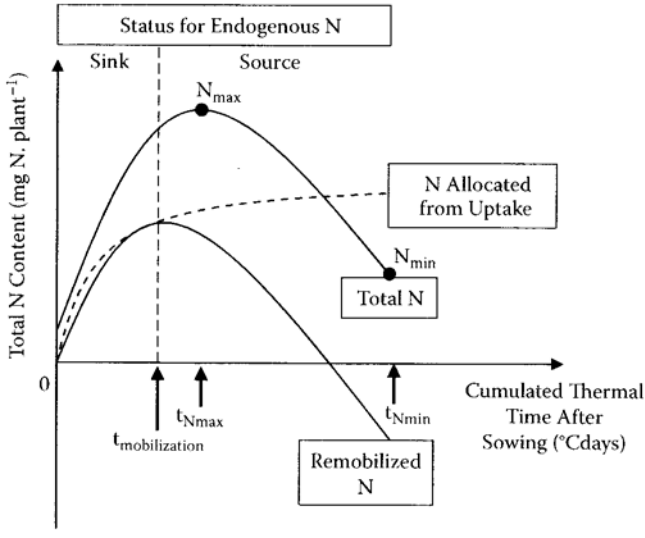


FIGURE 3.6 Conceptual description of N dynamics in each organ during source/sink transition by parameters characterizing N allocation and N mobilization. t_{Nmax} and t_{Nmin}: time when total N content (mg·plant^{-1}) is maximal and minimal, respectively; N_{max} and N_{min}: maximal and minimal total N content value (mg·plant^{-1}); $t_{mobilization}$: time when endogenous N mobilization starts. [Redrawn from Malagoli et al. (2005b).

N mobilized when each organ switches to a source status for N. Balance of these fluxes describes the sink–source transition that may occur, as described in Figure 3.6, for all compartments of the plant, and particularly for leaves. Malagoli et al. (2005b) have successfully modeled this system to have access to a highly mobile N pool (circulating amino acids, peptides, and other N translocation forms) that may behave as a signal for regulation of root N uptake (Forde 2002). In a second step, the effect of environmental changes (mostly light and temperature) has been studied to explain the capacity of the leaves to efficiently remobilize N. Such an approach has been used to understand how the canopy/morphogenesis of a given genotype will affect the local environment and subsequent leaf senescence and, consequently, the level of N remobilization to the seeds (Gombert et al. 2006).

3.4 CONCLUSION

The use of equations describing the kinetics of NO_3^- high- and low-affinity transport systems, HATS and LATS, respectively, and of the oilseed rape plant databank from INRA (providing inputs and outputs needed to run the model) facilitated the development of a basic mechanistic N-uptake model during the growth cycle. Characterization of endogenous (day/night cycle, ontogeny) and environmental (root temperature and photosynthetically active radiation) factors on transport system activities by ^{15}N-labeling experiments allowed the development of response curves. Integration of these factors led to the development of a model to quantify the impact of each studied factor, as well as the relative contribution of each transport system during the growth cycle. Simulations showed that HATS represents 89% of N taken

up at harvest (71% and 18% for inducible and constitutive components of HATS, respectively) when no fertilizer was applied. LATS activity occurred early in the growth cycle. A fall N-fertilizer application increased both its duration of function and its contribution to total N uptake.

Weekly application of ^{15}N on individual plants under field conditions made it possible to discriminate N flux coming from current N uptake (labeled N) and N remobilization (unlabeled N) between each tissue from bolting to harvest. In our conditions, endogenous N coming from N mobilized from vegetative tissues represents the main N source for N pod filling (73% of total N allocated toward pods at harvest, with 36%, 34%, 22%, and 8% coming from leaves, stem, flowers, and taproot, respectively). Despite a decrease of N uptake occurring during the flowering period and associated with an increase of the endogenous N pool circulating at the whole-plant level, no correlation was clearly found between N uptake and N remobilization. In conclusion, our results showed that this macroelement is submitted to a complex dynamic within the plant, thereby opening new research areas in an effort to optimize the utilization of nitrogen by this crop.

It appears that optimization of both the N fertilization rate and schedule, combined with a genetic improvement of the N harvest index in winter oilseed rape, are probably the most readily available tools to improve the yield of this crop while minimizing N release to the environment. Accordingly, a better understanding of N uptake and N partitioning, along with the contribution of these key physiological processes to biomass and yield formation, is required as a basis for genetic improvement. However, genotypic characteristics are difficult to estimate due to the large interaction between genotype and the environment. The ultimate aim of our work is to discriminate genotypic responses in N efficiency and to what extent they are modulated by environmental changes and the availability of nitrogen resources. This approach will be helpful in identifying relevant indicators and, further, breeding plants with higher efficiency to mobilize N toward harvested tissues in N-limiting soil conditions. A simulation with the compartmental model based on N allocation and remobilization within the plant indicated that a drop of dead leaves with a N content as low as 1% DW would increase either seed yield or N content by 15%. Our work, now in progress, will strive to understand how efficient N uptake and/or remobilization levels to the seeds will be affected in contrasting genotypes differing by their shoot or even root architecture.

REFERENCES

Beuve, N., N. Rispail, P. Lainé, J. B. Cliquet, A. Ourry, and E. Le Deunff. 2004. Putative role of aminobutyric acid (GABA) as a long distance signal in up-regulation of nitrate uptake in *Brassica napus* L. *Plant Cell Environ.* 27: 1035–1045.

Boelcke, B., J. Leon, R. R. Shulz, G. Shroder, and W. Diepenbrock. 1991. Yield stability of winter oil-seed rape (*Brassica napus* L.) as affected by stand establishment and nitrogen fertilization. *J. Agron. Crop Sci.* 167:241–248.

Britto, D. T., and H. J. Kronzucker. 2002. NH_4^+ toxicity in higher plants: A critical review. *J. Plant Physiol.* 159: 567–584.

Chapman, J. F., D. H. Scarisbrick, and R. W. Daniels. 1984. Field studies on ^{14}C assimilate fixation and movement in oil-seed rape (*Brassica napus* L.). *J. Agric. Sci.* 102: 23–31.

Clement, C. R., M. J. Hopper, R. J. Canaway, and P. P. H. Jones. 1974. A system for measuring the uptake of ions by plants from solutions of controlled composition. *J. Exp. Bot.* 25: 81–99.

Faure-Rabasse, S., E. Le Deunff, P. Lainé, J. H. Macduff, and A. Ourry. 2002. Effects of nitrate pulses on *BnNRT1* and *BnNRT2* genes mRNA levels and nitrate influx rates in relation to the duration of N deprivation in *Brassica napus* L. *J. Exp. Bot.* 53: 1711–1721.

Forde, B. G. 2002. Local and long-range signalling pathways regulating plant responses to nitrate. *Annu. Rev. Plant Biol.* 53: 203–224.

Fraisier, V., M. F. Dorbe, and F. Daniel-Vedele. 2001. Identification and expression analysis of two genes encoding putative low-affinity nitrate transporters from *Nicotiana plumbaginifolia*. *Plant Mol. Biol.* 45: 181–190.

Gabrielle, B., P. Denoroy, G. Gosse, E. Justes, and M. N. Andersen. 1998. Development and evaluation of a CERES-type model for winter oilseed rape. *Field Crops Res.* 57: 95–111.

Gombert, J., P. Etienne, A. Ourry, and F. Le Dily. 2006. The expressions patterns of *SAG12/Cab* genes reveal the spatial and temporal progression of leaf senescence in *Brassica napus* L. with sensitivity to the environment. *J. Exp. Bot.* 57: 1949–1956.

Gosse, G., P. Cellier, P. Denoroy, B. Gabrielle, P. Laville, B. Leviel, E. Justes, B. Nicolardot, B. Mary, S. Recous, J. C. Germon, C. Hénault, and P. K. Leech. 1999. Water, carbon and nitrogen cycling in a rendzina soil cropped with winter rape: The Châlons oilseed rape database. *Agronomie* 19: 119–124.

Hatch, D. J., M. J. H. Hopper, and M. S. Dhanoa. 1986. Measurement of ammonium ions in flowing solution culture and diurnal variation in uptake in *Lolium perenne*. *J. Exp. Bot.* 37: 589–596.

Huang, N. C., K. H. Liu, H. J. Lo, and Y. F. Tsay. 1999. Cloning and functional characterization of an *Arabidopsis* nitrate transporter gene that encodes a constitutive component of low-affinity uptake. *Plant Cell* 11: 1381–1392.

Lainé, P., A. Ourry, J. Macduff, J. Boucaud, and J. Salette. 2002. Kinetic parameters of nitrate uptake by different catch crop species: Effect of low-temperatures or previous nitrate starvation. *Physiol. Plant.* 88: 85–92.

Liu, K. H., C. Y. Huaug, and Y. F. Tsay. 1999. CHL1 is a dual-affinity nitrate transporter of *Arabidopsis* involved in multiple phases of nitrate uptake. *Plant Cell* 11: 865–874.

Malagoli, P., P. Lainé, E. Le Deunff, L. Rossato, B. Ney, and A. Ourry. 2004. Modeling N uptake in *Brassica napus* L. cv. Capitol during the growth cycle using influx kinetics of nitrate transport systems and field experimental data. *Plant Physiol.* 134: 388–400.

Malagoli, P., P. Lainé, L. Rossato, and A. Ourry. 2005a. Dynamics of nitrogen uptake and mobilization in field-grown winter oilseed rape from bolting to harvest. I: Global N flows between vegetative and reproductive tissues in relation to leaf fall and their residual N. *Ann. Bot.* 95: 853–861.

Malagoli, P., P. Lainé, L. Rossato, and A. Ourry. 2005b. Dynamics of nitrogen uptake and mobilization in field-grown winter oilseed rape from bolting to harvest. 2: A ^{15}N-labelling-based simulation model of N partitioning between vegetative and reproductive tissues. *Ann. Bot.* 95: 1187–1198.

Mendham, N. J., P. J. Shipway, and R. K. Scott. 1981. The effects of delayed sowing and weather on growth, development and yield of winter oil-seed rape (*Brassica napus*). *J. Agric. Sci.* 96: 417–428.

Noquet, C., J.-C. Avice, L. Rossato, P. Beauclair, M.-P. Henry, and A. Ourry. 2003. Effects of altered source-sink relationships on N allocation and vegetative storage protein in accumulation in *Brassica napus* L. *Plant Sci.* 166: 1007–1018.

Ono, F., W. B. Frommer, and N. von Wiren. 2000. Coordinated diurnal regulation of low- and high-affinity nitrate transporters in tomato. *Plant Biol.* 2: 17–23.

Redinbaugh, M. G., and W. H. Campbell. 1991. Higher plant responses to environmental nitrate. *Physiol. Plant.* 82: 640–650.

Schjoerring, J. K., J. G. H. Bock, L. Gammelvind, C. R. Jensen, and V. O. Mogensen. 1995. Nitrogen incorporation and remobilization in different shoot components of field-grown winter rape (*Brassica napus* L.) as affected by rate of nitrogen application and irrigation. *Plant Soil* 177: 255–264.

Sieling, K., and O. Christen. 2001. Effect of preceding crop combination and N fertilization on yield of six oil-seed rape cultivars (*Brassica napus* L.). *Eur. J. Agron.* 7: 301–306.

Touraine, B., F. Daniele-Vedele, and B. Forde. 2001. Nitrate uptake and its regulation. In *Plant nitrogen*, ed. P. J. Lea and J. F. Morot-Gaudry, 1–37. Berlin: Springer-Verlag.

Wang, R., D. Liu, and N. M. Crawford. 1998. The *Arabidopsis* CHL1 protein plays a major role in high-affinity nitrate uptake. *Proc. Natl. Acad. Sci.* 95: 15134–15139.